ECOLE
POLYTECHNIQUE
DE BRUXELLES

Université Libre de Bruxelles

Summary

Aerodynamics
MECA-Y-402

Author:
Enes Ulusoy

Professor:
Herman Deconinck

Year 2016 - 2017

Appel à contribution

Synthèse Open Source

Ce document est grandement inspiré de l'excellent cours donné par Herman Deconinck à l'EPB (École Polytechnique de Bruxelles), faculté de l'ULB (Université Libre de Bruxelles). Il est écrit par les auteurs susnommés avec l'aide de tous les autres étudiants et votre aide est la bienvenue ! En effet, il y a toujours moyen de l'améliorer surtout que si le cours change, la synthèse doit être changée en conséquence. On peut retrouver le code source à l'adresse suivante

`https://github.com/nenglebert/Syntheses`

Pour contribuer à cette synthèse, il vous suffira de créer un compte sur *Github.com*. De légères modifications (petites coquilles, orthographe, ...) peuvent directement être faites sur le site ! Vous avez vu une petite faute ? Si oui, la corriger de cette façon ne prendra que quelques secondes, une bonne raison de le faire !

Pour de plus longues modifications, il est intéressant de disposer des fichiers : il vous faudra pour cela installer LaTeX, mais aussi *git*. Si cela pose problème, nous sommes évidemment ouverts à des contributeurs envoyant leur changement par mail ou n'importe quel autre moyen.

Le lien donné ci-dessus contient aussi un `README` contenant de plus amples informations, vous êtes invités à le lire si vous voulez faire avancer ce projet !

Licence Creative Commons

Le contenu de ce document est sous la licence Creative Commons : *Attribution-NonCommercial-ShareAlike 4.0 International (CC BY-NC-SA 4.0)*. Celle-ci vous autorise à l'exploiter pleinement, compte- tenu de trois choses :

1. *Attribution* ; si vous utilisez/modifiez ce document vous devez signaler le(s) nom(s) de(s) auteur(s).
2. *Non Commercial* ; interdiction de tirer un profit commercial de l'œuvre sans autorisation de l'auteur
3. *Share alike* ; partage de l'œuvre, avec obligation de rediffuser selon la même licence ou une licence similaire

Si vous voulez en savoir plus sur cette licence :

`http://creativecommons.org/licenses/by-nc-sa/4.0/`

Merci !

Contents

Chapter 1

Aerodynamic Force

1.1 Derivation of the conservation laws

1.1.1 Mass conservation

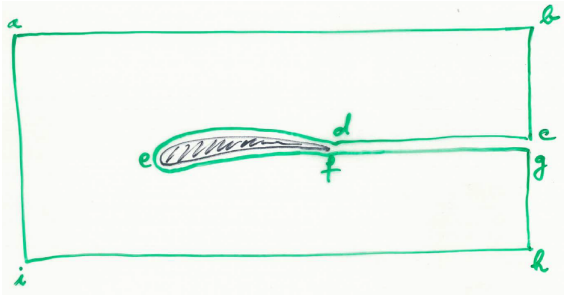

Figure 1.1

Consider the closed control volume S* (abhi) around the airfoil. It is a 2D view, but imagine that we have a 3D configuration with Z axis perpendicular to the sheet. Be aware that the normal is always perpendicular to the contour and is external! The fundamental integral form of the mass conservation equation is:

$$\frac{d}{dt}\int_V \rho\, dV + \oint_S \rho\vec{v}\, d\vec{S} = 0. \tag{1.1}$$

By applying Gauss theorem $\oint_S \vec{a}.\vec{n}\, dS = \int_V \nabla\vec{a}\, dV$, and regrouping the term in a unique integral, we obtain:

$$\int_V \left[\frac{d\rho}{dt} + \nabla.(\rho\vec{v})\right] dV = 0. \tag{1.2}$$

Considering this to be true for all volumes, the integral disappear and gives the

Continuity equation

$$\frac{d\rho}{dt} + \nabla.(\rho\vec{u}) = 0 \tag{1.3}$$

Another form can be found by introducing the material derivative $\dot{\rho} = \frac{d\rho}{dt} + (\vec{v}.\nabla)\rho$, and if we are in a steady state, the time derivative goes away.

1.1.2 Momentum equation

The general form of the momentum equation is:

$$\rho\dot{\vec{v}} = \frac{\partial\rho\vec{v}}{\partial t} + \rho(\vec{v}\nabla)\vec{v} = -\nabla p + \nabla\bar{\bar{\tau}}. \tag{1.4}$$

By considering a steady state, the time derivative goes away. If we consider the x component of the velocity, we can expend the derivative to the whole left term as:

$$\rho(\vec{v}\nabla)v_x = \nabla(\rho\vec{v}v_x) - v_x\cancel{\nabla(\rho\vec{v})} \tag{1.5}$$

where the last term is null related to (1.3) in steady state. Integrating both sides around the volume contained in the closed surface S (abcdefghi on figure) in (1.5), and applying Gauss theorem, we obtain:

$$\oint_S \vec{v}(\rho\vec{v}\vec{n})\,dS = -\oint_S p\,d\vec{S} + \oint_S \bar{\bar{\tau}}\,d\vec{S}. \tag{1.6}$$

Let's now apply this equation to the new closed contour $S* = S - \text{airfoil} - cd - fg$ (previous abhi in fact). (1.6) becomes:

$$\begin{aligned}&\oint_{S^*} \vec{v}(\rho\vec{v}\,d\vec{S}) + \cancel{\oint_{\text{airfoil}} \vec{v}(\rho\vec{v}\,d\vec{S})} + \cancel{\oint_{cd+fg} \vec{v}(\rho\vec{v}\,d\vec{S})}\\ &= -\oint_{S^*} p\,d\vec{S} - \oint_{\text{airfoil}} p\,d\vec{S} - \cancel{\oint_{cd+fg} p\,d\vec{S}} + \oint_{S^*} \bar{\bar{\tau}}\,d\vec{S} + \oint_{\text{airfoil}} \bar{\bar{\tau}}\,d\vec{S} + \cancel{\oint_{cd+fg} \bar{\bar{\tau}}\,d\vec{S}}\end{aligned} \tag{1.7}$$

where the $cd + fg$ components cancels each other if we consider that they are infinitely close to each other, as they are opposite. The airfoil integral in the left hand side is null because the wing can not be penetrated by the flow. If we manipulate the equation to refind the (1.6) shape by regrouping airfoil terms in an additional $\vec{R}$ term. Taking account the orientation of normals, the signs will be chosen in the way $\vec{R}$ is a

Force applied on the wing

$$\vec{R} = \oint_{\text{airfoil}} p\,d\vec{S} - \oint_{\text{airfoil}} \bar{\bar{\tau}}\,d\vec{S} \tag{1.8}$$

so that (1.7) becomes, after considering S* to be a contour in the **far field** so that viscous effects vanish (to avoid other parameters calculation):

$$\oint_{S^*} \vec{v}(\rho\vec{v}\,d\vec{S}) = -\oint_{S^*} p\,d\vec{S} + \cancel{\oint_{S^*} \bar{\bar{\tau}}\,d\vec{S}} - \vec{R}. \tag{1.9}$$

We still have to measure the pressure.

Uniform p along S*

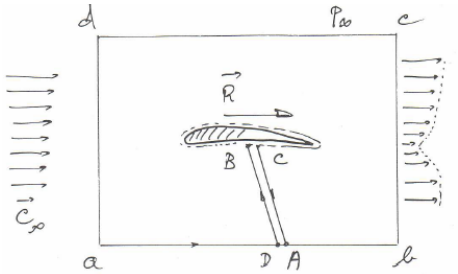

Figure 1.2

By considering this (assumption of far field), we can compute the force only by knowing the far field parameters. Indeed, uniform pressure implies null surface integral, so that (1.9) becomes:

$$\vec{R} = -\oint_{S^*} \vec{v}(\rho\vec{v}\,d\vec{S}). \tag{1.10}$$

The velocity term remains, as by experience we know that there is a **wake** making the velocity profile non-uniform. Let's now consider that the velocity is horizontal so that $\vec{R} = R.\vec{1}_x$, at the inlet we have $\vec{v}$ and $\vec{n}$ are opposed while at the outlet they are in the same direction:

$$\vec{R} = \int_a^d \vec{v}\,d\dot{m} - \int_b^e \vec{v}\,d\dot{m} > 0 \tag{1.11}$$

showing that there is only **drag** force.

1.2 The aerodynamic lift

We know in practice that there is also a lift force. In fact, the assumption of uniform pressure is wrong because the pressure effects induced by the body remains at a long distance from the body. We have to analyse the **non uniform** p along S*. In order to apply Bernouilli equation $p + \frac{1}{2}\rho v^2 = cst$, let's add the constants p_∞ and v_∞ to (1.9), as $\oint p_\infty \, d\vec{S} = p_\infty \oint d\vec{s} = 0$:

$$\vec{R} = -\oint_{S^*} (p - p_\infty)\, d\vec{S} - \oint_{S^*} (\vec{v} - \vec{v}_\infty)\, d\dot{m} \tag{1.12}$$

Let's express $\vec{v} = \vec{v}_\infty + \vec{\delta_c}$ with $\vec{\delta_c}$ a perturbation. Introducing this in Bernouilli equation:

$$\begin{aligned} p_\infty + \frac{1}{2}\rho\cancel{\vec{v}_\infty^{\,2}} = p + \frac{1}{2}\rho(\vec{v}_\infty + \vec{\delta_c})^2 = p + \frac{1}{2}\rho(\cancel{\vec{v}_\infty^{\,2}} + 2\vec{v}_\infty\vec{\delta_c} + \cancel{\vec{\delta_c}^{\,2}}) \\ \Rightarrow p - p_\infty = -\rho\vec{v}_\infty\vec{\delta_c}. \end{aligned} \tag{1.13}$$

If we replace this result in (1.12), we find:

$$\begin{aligned} \vec{R} &= \oint_{S^*} \rho(\vec{v}_\infty\vec{\delta_c})\, d\vec{S} - \oint_{S^*} \rho\vec{\delta_c}[(\vec{v}_\infty + \cancel{\vec{\delta_c}})\, d\vec{S}] \\ &= \oint_{S^*} \rho[(\vec{v}_\infty\vec{\delta_c})\, d\vec{S} - \vec{\delta_c}[(\vec{v}_\infty . d\vec{S})] \end{aligned} \tag{1.14}$$

by using a vector property $\vec{a} \times (\vec{b} \times \vec{c}) = (\vec{a}\vec{b})\vec{c} - (\vec{a}\vec{c})\vec{b}$:

$$= \rho\vec{v}_\infty \times \oint_{S^*} \vec{\delta_c} \times d\vec{S} = \rho\vec{v}_\infty \times \left[\oint_{S^*} \vec{v} \times d\vec{S} - \cancel{\oint_{S^*} \vec{v}_\infty \times d\vec{S}}\right] \tag{1.15}$$

and by applying Stokes theorem $\oint_S \vec{a} \times d\vec{S} = \int_V \nabla \times \vec{a}\, dV$:

$$= \rho\vec{v}_\infty \times \int (\nabla \times \vec{v})\, dV = \rho\vec{v}_\infty \times \int \vec{w}\, dV \tag{1.16}$$

where $\vec{w}$ is the **vorticity vector** of direction $\vec{1}_z$ (pointing in the paper):

$$\vec{w} = \begin{vmatrix} \vec{1}_x & \vec{1}_y & \vec{1}_z \\ \partial_x & \partial_y & 0 \\ v_x & v_y & 0 \end{vmatrix} = [\partial_x v_y - \partial_y v_x]\vec{1}_z \tag{1.17}$$

This shows that the lift force is always perpendicular to the flow!

1.3 The Kutta-Joukowski formula

We will now introduce the circulation $\Gamma = -\oint \vec{v}\, d\vec{l} > 0$ around a body. The convention is to take the anticlockwise direction for $d\vec{l}$ and so for Γ to be > 0 we must have $\vec{v}$ in the clockwise direction. There is a link between the lift force and the circulation. Let's introduce **Stokes theorem**:

$$\oint \vec{a} d\vec{l} = \int_S (\nabla \times \vec{a})\, d\vec{S} \qquad \Rightarrow -\Gamma = \int_S \vec{w} d\vec{S}. \tag{1.18}$$

We remember that:

$$\begin{aligned} &\vec{R} = \rho\vec{v}_\infty \times \int \vec{w}\, dV = \rho\vec{v}_\infty \times \int l\vec{w}\, dS \qquad \Leftrightarrow \frac{\vec{R}}{l} = \rho\vec{v}_\infty \times \int \vec{w}\, dS \\ &\frac{\vec{R}}{l} = \rho\vec{v}_\infty \times \int \vec{w}\, (d\vec{S}.\vec{1}_z) = \rho\vec{v}_\infty \times (-\Gamma)\vec{1}_z = \rho v_\infty \Gamma\, \vec{1}_y \end{aligned} \tag{1.19}$$

to finally obtain a very good approximation of the lift:

Kutta formula for lift 2D airfoil

$$|R| = \rho v_\infty \Gamma \tag{1.20}$$

Application to airfoils

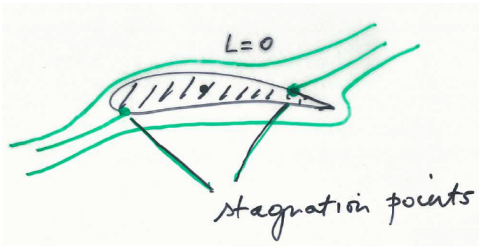

Figure 1.3

In inviscid case, the Kelvin theorem states that there cannot be vorticity, so no lift. If we take an arbitrary contour around the airfoil we will have no circultion. In inviscid case we can never get a lift → D'alembert paradox. At the trailing edge, if the flow wants to continue on the other corner from below, the velocity must be infinity so that the flow separates. But this is not the case in reality.

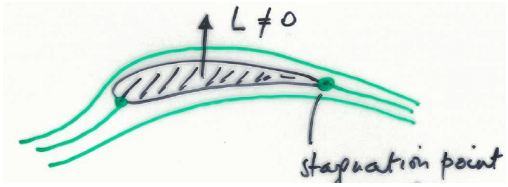

Figure 1.4

After some processes we can obtain the stagnation point on the trailing edge so that we satisfy the Kutta condition (the flow has to leave the airfoil smoothly). So in this case, there is a circulation if we take a contour that contains the airfoil, but for all contour that does not contain the airfoil it is null. But why to put the stagnation point at the trailing edge? This is purely physics. Γ varies with the stagnation point position, but only one corresponds to the Kutta condition.

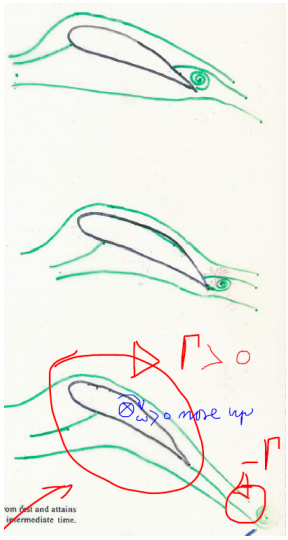

Figure 1.5

What happens is that initially we have the first kind of flow, then the formation of the starting vortex due to viscous effects (separation) which is compensated by a **bound vortex** around the airfoil (to respect Kelvin theorem of irrotational flow) that makes $\Gamma \neq 0$. Then the vortex goes away to infinity. Indeed if we take $R = \rho v_\infty \Gamma$, $\Gamma \neq 0$, so we have lift.

We can show that every contour containing the airfoil has a non 0 circulation. Let's proof that a contour that doesn't contain the airfowl has $\Gamma = 0$:

ADD FIGURE (1)

$$\oint_C \vec{v}\, d\vec{l} = \oint_{\text{airfoil}} \vec{v}\, d\vec{l} + \oint_{cd} \vec{v}\, d\vec{l} + \oint_{fg} \vec{v}\, d\vec{l} = 0. \tag{1.21}$$

As the contour elements are exactly opposed to each other, the result is null.

Chapter 2

The 2D airfoil

2.1 Nomenclature

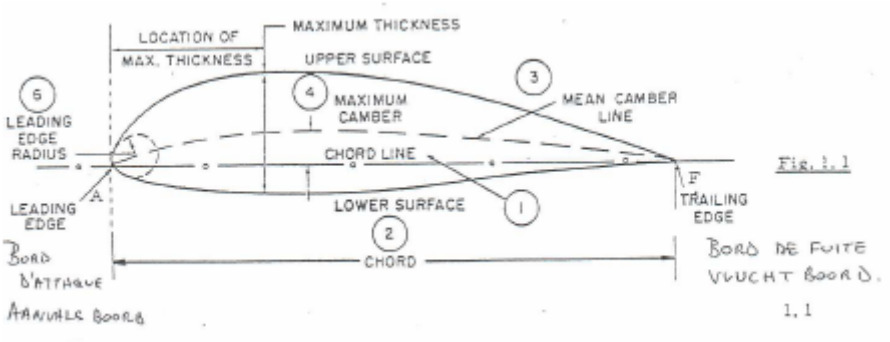

Figure 2.1

The connection between the trailing edge and the leading edge is called the **chord**. Then we have a **camber line** which is the line following the shape of the airfoil and characterizing the geometry. The leading and trailing edges are respectively the starting and ending point of the camber line. The thickness is always normal to the camber line. Let's note that the camber line and the thickness distribution are function of the position $f(x)$.

Eastman Jacobs created around 1930 a family of wing profiles, known as the NACA profiles. He characterised them by 4 digit numbers:

- The first is the **maximum camber in percentage of the chord**
- The second is the **position of the maximum camber in 1/10 percentage of the chord**
- The last two digits gives the **position of the maximum thickness in percentage of the chord**

These were characterizing the 2D representation, but a wing is 3D. We have also the **wing surface S**, **the span of the wing b** and we can define a mean chord when this last is not constant as:

$$< c >= \frac{S}{b}. \tag{2.1}$$

For civil aircraft, b/c is between 6-10 and for glider b/c = 12, this is called the **aspect ratio** (slenderness ratio).

2.2 The flow around 2D airfoils

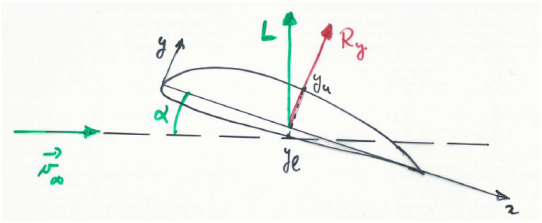

Figure 2.2

Let's remind the expression of the force applied on the wing:

$$\vec{R} = -\oint p\, d\vec{S} + \oint \bar{\bar{\tau}}\, d\vec{S} \tag{2.2}$$

with an external normal to the airfoil. The angle of attack is represented on Figure 2.2.
The pressure term is responsible for lift and the friction term is responsible for drag. Friction forces work tangential to the airfoil and the pressure forces are perpendicular, if there is **no separation** in the flow. The drag created by the stress is called the **skin** or **friction** drag. Note that in a subsonic inviscid incompressible flow, we have the paradox of d'Alembert because we have no drag. This shows that the pressure only contributes to lift.

What happens when we have **separation** is that we have a region above the airfoil where $p - p_\infty \approx 0$ and so we have a very big pressure below $p \gg p_\infty$ that slows down the wing. This implies that the applied force is higher than the case without separation and due to the attack angle, the drag force too. This phenomenon is called **pressure drag** (form drag), and here the pressure contributes to drag.

ADD FIGURE 4

The figure shows how the geometry of the body influence the drag force which can be sometimes principally caused by pressure. If we have a flat plate or a cylinder we have a huge separation, so principally a form drag D_f. We will have less pressure drop with the wing profile as it perfectly follows the flow direction, to end up smoothly, in this case the friction drag D_f is more important. This shows the importance of profiles.

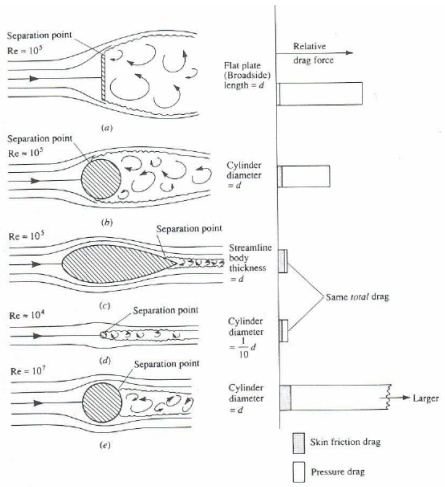

Figure 2.3

If we look to the weight of a plane, it is surprising to see the importance of lift force. This is possible thanks to the high **atmospheric pressure**. Indeed, the wing load is defined as:

$$\text{wing load} = \frac{\text{weight plane}}{\text{surface aera wings}} \tag{2.3}$$

and this is commonly approximately equal to 5000 Pa = 500 kg/m^2. This can be easely reached by a small perturbation of the atmospheric pressure (10^5Pa $\rightarrow$ 5% = 5000 Pa).

2.2.1 Distribution of the pressure coefficient

Let's see the effect of the angle of attack. For small angles, we can neglect the force derivation implied and consider it to be perpendicular to the chord. This allows to neglect the

drag component (refer to Figure 2.2). If we assume that v is in the x direction, the lift force approximation is:

$$R_y = -\oint p\, d\vec{S}.\vec{1}_y = -\oint p\, dS_y. \tag{2.4}$$

The lift force is fully created by pressure and we can call the lower part of the wing the **pressure side** and the upper part the **suction side**.

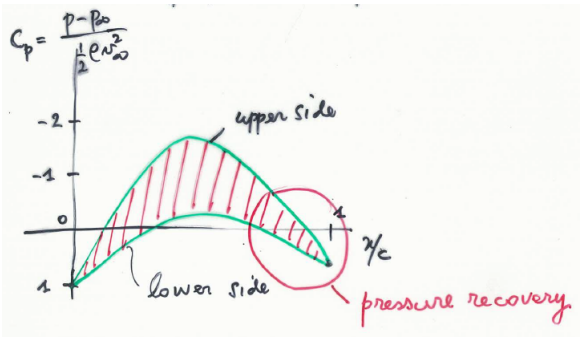

Figure 2.4

The suction effect is always bigger than the pressure one. We introduce the pressure coefficient $C_p = \frac{p-p_\infty}{\frac{1}{2}\rho v_\infty^2}$ which direction points always down! The pressure side is the green curve below and the suction side is the green curve on the upper side of Figure 2.4.

If we look to the leading edge, we have a tendency to go to $C_p = 1$. Indeed, if we write Bernouilli along a streamline and take into account the stagnation point where $v = 0$, we have:

$$p_\infty + \rho\frac{v_\infty^2}{2} = cst = p_{LE} + 0 \qquad \Rightarrow C_p = \frac{p_{LE} - p_\infty}{\frac{1}{2}\rho v_\infty^2} = 1. \tag{2.5}$$

The pressure recovery means that we will have again $p = p_\infty$ at that point. At the leading edge this is the case because it is commonly a stagnation point.

For the trailing edge we have two cases. If it is **blunt** trailing edge, we have the $C_p = 1$ case (leading edge always blunt). If we have a **sharp** trailing edge, we will have v_∞ at the previous stagnation point and so the Bernouilli equation rewrites:

$$p_\infty + \rho\frac{v_\infty^2}{2} = cst = p_{TE} + \rho\frac{v_\infty^2}{2} \qquad \Rightarrow C_p = \frac{p_{TE} - p_\infty}{\frac{1}{2}\rho v_\infty^2} = 0. \tag{2.6}$$

We have a very big expansion on the LE (separation), so this induces a suction peak as the pressure falls above and increases below. Then we go back to the normal pressure. Let's remind that decreasing pressure is favourable because the flow stays attached but if we have pressure increase, it's unfavourable, because we risk separation. The angle of attack is important because the flow has more difficulties to turn on the LE when angle goes up so the separation and the sucking peak are more important.

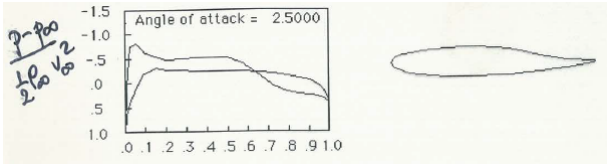

Figure 2.5

This case is particular because the rear is reversed, so the pressure side becomes sucking and inversely. The reduced camber and reduced thickness makes the wing more vulnerable to angle change.

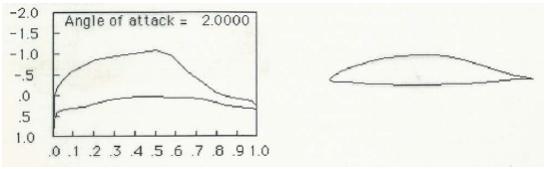

Figure 2.6

Natural laminar section. The smoother LE reduces the peak and the sharp TE induces $C_p = 0$.

This is a symetrical shape and thus only one line is shown. The thickness makes it more resistible to angle change.

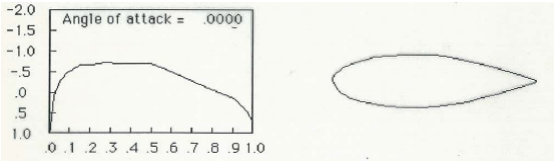

Figure 2.7

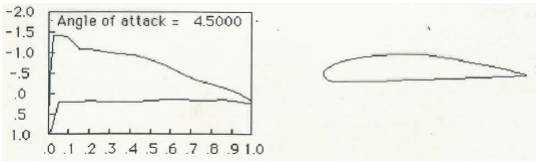

Figure 2.8

Even if the wing is thin, the camber makes it more suited to high attack angle.

2.3 Center of pressure, moment and aerodynamic center

2.3.1 Center of pressure and moment

Calculation of lift force

We can calculate the lift by $L = \rho v_\infty \Gamma$, but we need the Γ which is not calculable. So we will use the trick that consist in forgetting the drag term in the $\vec{R}$. Then we integrate the pressure around the surface:

$$\vec{R} = -\oint p\, d\vec{S} = -\sum \underbrace{p_i \Delta \vec{S}_i}_{\Delta R_i} \tag{2.7}$$

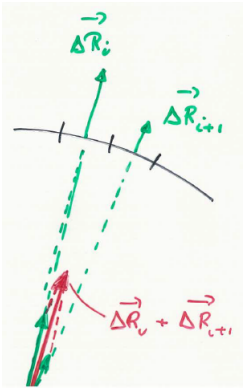

Figure 2.9

Center of pressure

It's the x value on the chord where the carrier of the force $\vec{R}$ intersects the chord. It's function of the angle of attack. Indeed, if alpha increases, the suction peak will be higher, this induces that the center of pressure move forward (participation of the forward pressure more important).

Note that the center of pressure is not a fixed point. Indeed, it varies with the angle of attack: if $\alpha \nearrow$, the pressure peak on the LE is more important making the x_p move upstream, and the contrary for $\alpha \searrow$. This notion will be completed by the **zero lift angle** α_0.

Equivalent forces

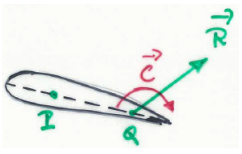

Figure 2.10

The force at the pressure center P is equivalent to another force in point Q, but by adding the moment to compensate the one added by moving the force. This moment is:

$$\vec{C_Q} = -\vec{PQ} \times \vec{R}. \tag{2.8}$$

Aerodynamic center

Suppose that there is a point Q where this couple C_Q is independent of the angle of attack (because the pressure center changes with alpha). This point is called the aerodynamic center. We have to show that this exists. For this way:

1. We will begin by calculating the center of pressure by integrating the pressure field. We can calculate the magnitude, but not the acting point.

2. We compute the momentum of the pressure forces around the leading edge (Figure 2.11):

$$\vec{M}_{LE} = \oint \vec{OQ} \times d\vec{F} = \underbrace{M_{LE}}_{<0} \vec{1}_z \tag{2.9}$$

   where $\vec{1}_z$ goes in the paper.
3. On the other hand, we know that $\vec{R}$ has a certain direction with a normal component, so we can make the moment (Figure 2.12):

$$M_{LE} = -x_p.N \tag{2.10}$$

By using point 2 and 3 we can find x_p.

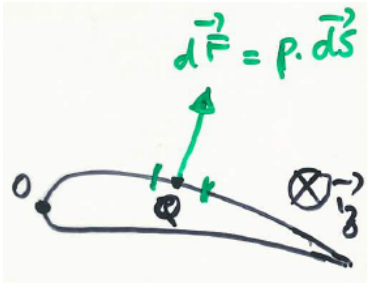

Figure 2.11

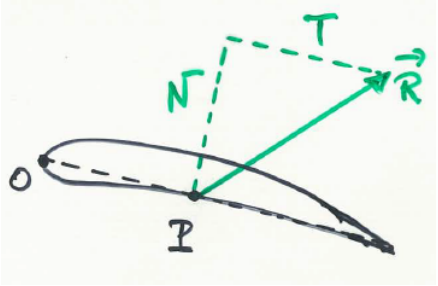

Figure 2.12

2.3.2 Aerodynamic center

Let's now be interested in how the the moment on a point Q on the wing varies with α. It is shown experimentally that:

$$c_m(Q) = c_{m_0} + kc_l \tag{2.11}$$

where c_m, c_l are respectively the non-dimensional moment and lift, and c_{m_0} the non-dimensional moment at zero lift. k is a constant that is related to the reference point chosen. If Q is taken on the LE for example, increasing α will produce an increase of the lift and make the center of pressure move upstream. The L increase will compensate the moving x_p such that the moment becomes even more noose-down (more negative following $\vec{1}_z$) $\Rightarrow k < 0$ for a decrease in (2.11). The same reasoning applied on the trailing edge gives $k > 0$.

This shows that it exists a point where $k = 0$, called the **aerodynamic center**. According to (2.11), this point will have a constant moment whatever α. Indeed, we will show that $c_l = m(\alpha - \alpha_0)$ and so:

$$c_m(Q) = c_{m_0} + km(\alpha - \alpha_0) \qquad \Rightarrow c_m(Q) = c_{m_0}. \tag{2.12}$$

We can benefit from this equation to show that c_{m_0} is well the moment for $\alpha = \alpha_0$, the zero lift angle (negative, descending arrow). We will also later show that when we decrease the angle of attack beginning from a positive one to the zero lift angle, the x_p will go downstream till infinity away the trailing edge, with an infinitely small lift,. This means that we will always have a finite noose-down moment.

Taking the opposite case of beginning from negative value of α, we will have the same value since the lift force is negative and the x_p in infinity further away from the leading edge. The **moment at zero lift** is thus **negative**. The explanations lead to the figures below.

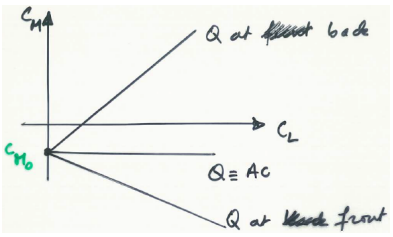

Figure 2.13

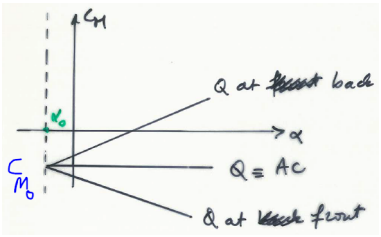

Figure 2.14

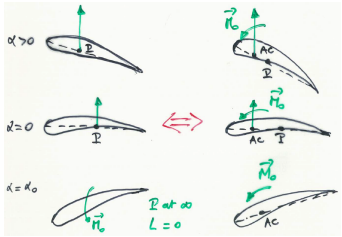

Figure 2.15

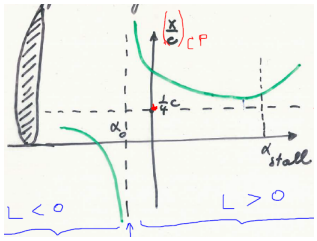

Figure 2.16

Let's finally establish the evolution of the pressure center in function of α. For this purpose, we need 4 equations:

$$\begin{array}{llll} 1) & c_m = c_{m_0} + kc_l & 2) & M_{ac} = (x_{ac} - x_{cp})N \\ 3) & m_{ac} = M_{AC} = M_0 < 0 & 4) & N = n(\alpha - \alpha_0) \end{array} \tag{2.13}$$

The AC being always upstream the CP the difference in 2) is < 0. In 4), $n > 0$. By using equation 3,4 and 2, we can compute:

$$M_0 = -(x_{cp} - x_{ac}).n(\alpha - \alpha_0) \quad \Leftrightarrow \quad -\frac{M_0}{n} = (x_{cp} - x_{ac}).(\alpha - \alpha_0) \tag{2.14}$$

This is the equation of an **hyperbola**. To see it, we only have to compute the limits of:

$$\begin{array}{ccc} & x_{cp} = x_{ac} - \frac{M_0}{n}\frac{1}{\alpha - \alpha_0} & \\ \lim_{\alpha \to \pm\infty} x_{cp} = x_{ac} & \lim_{\alpha \to \alpha_0 > 0} x_{cp} = +\infty & \lim_{\alpha \to \alpha_0 < 0} x_{cp} = -\infty \end{array} \tag{2.15}$$

The graph is shown on figure. Let's finally say that commonly, $x_{ac} = cst \approx \frac{1}{4}C$.

A particular case is the one of **symmetrical profile**. Indeed, in that case, the α_0 case correspond to $M_{ac} = 0$ and $L = 0$. The pressure center corresponds with the aerodynamic center and is **fixed**.

2.4 2D characteristics

2.4.1 Lift, drag and moment curves

Let's look to the non-dimensional parameters that will influence the lift;, the drag and the momentum. We have to define some reference quantities:

$$\begin{array}{cccc} L_{ref} = C & v_{ref} = v_\infty & t_{ref} = L_{ref}/v_{ref} & \rho_{ref} = \rho_\infty \\ t' = t/t_{ref} & p_{ref} = \rho_{ref}\frac{v_{ref}^2}{2} & \text{Mach} = V_{ref}/a_{ref} & a_{ref} = \gamma\pi T_{ref} \\ \gamma = c_p/c_v & & Re_{ref} = \frac{\rho_{ref} v_{ref} L_{ref}}{\mu_{ref}} & \end{array} \tag{2.16}$$

where a is the speed of sound. By replacing all these in the mass, momentum and energy equations, we obtain the non-dimensional ones (see Fluid Mechanics II):

$$
\begin{aligned}
&\bullet\ \frac{\partial \rho'}{\partial t'} + \nabla\left(\rho' \vec{v}'\right) = 0 \\
&\bullet\ \rho' \frac{d\vec{v}'}{dt'} = -\frac{1}{\gamma M_{ref}^2} \nabla p' + \frac{1}{\mathrm{Re}_{ref}} \nabla \bar{\bar{\tau}}' \\
&\bullet\ \frac{d}{dt'}(\rho' e') + \frac{\gamma(\gamma-1)}{2} M_{ref}^2 \frac{d}{dt'}(\rho' \vec{v}'^2) \\
&= \frac{\gamma}{Pr_{ref} Re_{ref}} \nabla(k' \nabla T') - (\gamma-1)\nabla(p' \vec{v}') + \gamma(\gamma-1)\frac{M_{ref}^2}{Re_{ref}} \nabla(\bar{\bar{\tau}}' \vec{v}')
\end{aligned}
\tag{2.17}
$$

We can see that a solution can only be function of 4 parameters: $M, Re, Pr = \frac{c_p \mu}{k}, \gamma$, but we know that the geometry and the angle of attack α have a role by means of the boundary conditions. Then, we assume that the fluid is air ($\gamma = 1.4$) and that we can neglect heat effects (no influence of Pr, incompressible and so low speed flows). The non-dimensional lift, drag and moment are thus function of M, Re, geometry and α. We can define **lift**, **drag** and **moment coefficient** as (we forget about compressibility $\rightarrow$ M, and Re effects are low for $C_L and C_M$):

$$
\begin{aligned}
C_L(\cancel{M}, \cancel{Re}, geometry, \alpha) &= \frac{L}{\frac{1}{2}\rho_{ref} v_{ref}^2 S} \\
C_D(\cancel{M}, Re, geometry, \alpha) &= \frac{D}{\frac{1}{2}\rho_{ref} v_{ref}^2 S} \\
C_M(\cancel{M}, \cancel{Re}, geometry, \alpha) &= \frac{M}{\frac{1}{2}\rho_{ref} v_{ref}^2 S c}
\end{aligned}
\tag{2.18}
$$

where L, D, M are the **dimensional** forces, c the mean chord (S/b) and S a reference surface (3D wing $\rightarrow$ total wing surface, 2D wing $\rightarrow$ S = c). We can experimentally show that the lift increases mainly linearly with α and the drag force is caused by friction effects and pressure differences involving with α. This gives the following equations (lower case for 2D):

$$
c_l = m(\alpha - \alpha_{L_0}) \qquad c_d = c_{d_0} + k c_l^2 \tag{2.19}
$$

where $m \approx 2\pi$ theoretically and 5.7 practically, k is a constant of order of magnitude 0.01.

2.4.2 Stall and critical angle of attack

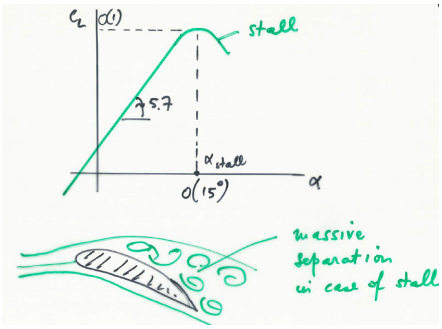

Figure 2.17

At a certain angle of attack ($\approx 15^\circ$), the lift suddenly drops. This is due to massive separation on the suction side (reverse pressure gradient too high) and happens at the **critical angle of attack**. This phenomenon is called **stall**. In the separated part, the pressure will no longer decrease and will form a pressure plateau.

We have to make the difference between leading-edge stall and trailing-edge stall. For **leading-edge stall**, the massive separation occurs suddenly near the LE resulting

in a strong and sudden drop of lift, when at maximum lift. This especially occurs to thin airfoils with cross-sections between 10 and 16% of the chord. For the **trailing-edge stall**, the point of separation gradually goes upstream with increasing angle of attack resulting in a more gradual drop of lift (more thick airfoils). The comparison is done on the right figure. We can also see a third type of stall called **thin airfoil stall** with the example of a flat plat.

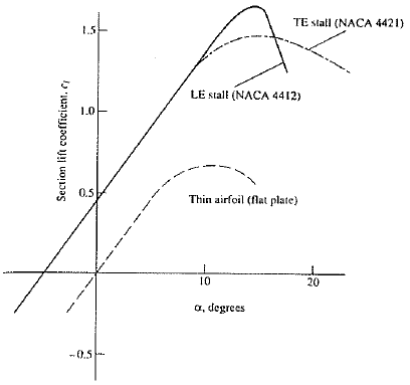

Figure 2.18

In conclusion, the LE must be sufficiently rounded to have a good maximum lift. In fact the profile may nor be too thick nor too thin. The figure on the left shows the influence of the thickness on the lift. We notice that the optimum thickness is situated around 12% of the chord.The maximum lift increases with RE, indeed higher the Re, higher is the ratio of speed versus viscosity. So we can better oppose to separation. Unlike the Re number, the roughness has great effects on the maximum lift. Finally, let's notice that the camber have also an effect on maximum lift, the best is a camber of 8 up to 10%.

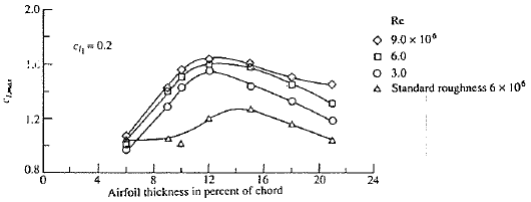

Figure 2.19

2.4.3 Maximum lift, stalling speed, polar curve and glide ratio

From C_L in (2.18), we can deduce the lift:

$$L = C_L \frac{1}{2} \rho_{ref} v_{ref}^2 S. \tag{2.20}$$

The lift force must always at least be equal to the weight of the plane. This implies that for low speed (take-off and landing), the C_L must be large. This is accomplished with large α and slats or flaps. The minimum speed where the lift can still balance the weight (C_L maximum) is called **stall speed** and from (2.20) we find:

$$v_{stall} = \sqrt{\frac{W}{C_{L_{max}} \frac{1}{2} \rho_{ref} S}} \tag{2.21}$$

The curve that represents C_L in function of C_D is the **polar curve** of the wing. The ratio $\frac{C_L}{C_D}$ is the **glide ratio** or **finesse** and is like an efficiency parameter. The best parameter is obtained using the graph by calculating β such that:

$$\tan \beta = \left(\frac{C_L}{C_D} \right)_{max} \tag{2.22}$$

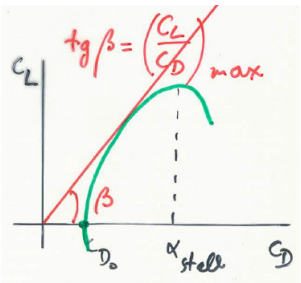

Figure 2.20

This point is important for the quality of the wing because if we plot the thrust, the lift, the drag and the weight of a plane describing a horizontal flight (Figure 2.21), the thrust is given by:

$$T = \frac{L}{\tan \beta} = \frac{W}{\tan \beta} \tag{2.23}$$

where we see that when $\tan\beta$ (so the glide ratio) increases, T decreases. Another interpretation can be given when we have no thrust (Figure 2.22). In this case the gliding ratio has to be adapted to travel the larger distance knowing that:

$$\frac{C_L}{C_D} = \frac{\text{distance travelled}}{\text{height loss}} \tag{2.24}$$

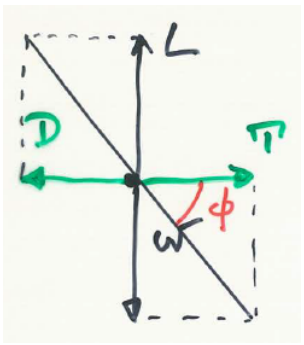

Figure 2.21

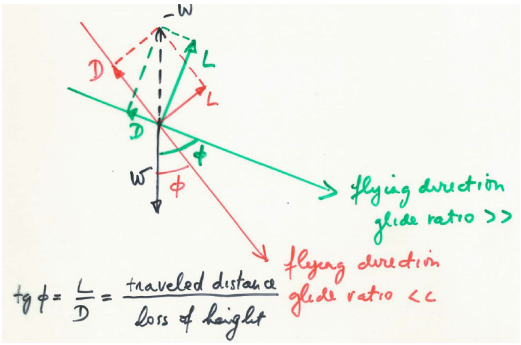

Figure 2.22

2.5 Methods to calculate flows around 2D airfoils

2.5.1 Conformal mapping

We will begin here with steady, inviscid irrotational flows. This gives for the mass conservation equation:

$$\frac{\partial\rho}{\partial t} + \nabla(\rho\vec{v}) = 0 \qquad \Rightarrow \nabla\vec{v} = 0 = \partial_x u + \partial_y v \tag{2.25}$$

In the other hand, we have the assumption of irrotational flow:

$$\vec{w} = 0 \qquad \Rightarrow \partial_x v - \partial_y u = 0. \tag{2.26}$$

Then we define the **complex potential functoin w**:

$$w = \phi + I\psi \tag{2.27}$$

where ϕ is the **potential function** (satisfies $w = 0$ by construction) such that:

$$\begin{cases} u = \partial_x\phi \\ v = \partial_y\phi \end{cases} \qquad \nabla\phi = \vec{v} = \partial_x\phi\vec{1}_x + \partial_y\phi\vec{1}_y \tag{2.28}$$

We must satisfy the mass conservation equation:

$$\nabla(\nabla\phi) = 0 \qquad \Rightarrow \Delta\phi = 0 \tag{2.29}$$

coupled with boundary conditions, we can find a solution $\phi(x, y)$. The **stream function** satisfies the mass conservation by construction:

$$\begin{cases} u = \partial_y\psi \\ v = -\partial_x\psi \end{cases} \qquad \Rightarrow \partial_x u + \partial_y v = 0 \Leftrightarrow \partial_x(\partial_y\psi) + \partial_y(-\partial_x\psi) = 0 \tag{2.30}$$

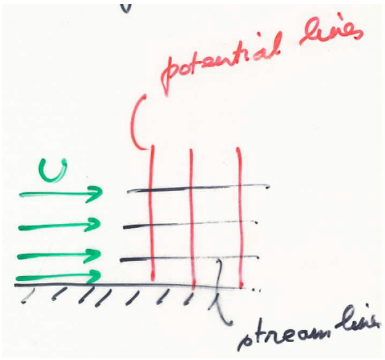

Figure 2.23

We still have to verify the $w = 0$ condition:

$$\partial_x v - \partial_y u = 0 \qquad \Rightarrow \frac{\partial^2 \psi}{\partial x^2} + \frac{\partial^2 \psi}{\partial y^2} = 0 \qquad \Delta\psi = 0 \qquad (2.31)$$

A streamline and a potential line are perpendicular to each other:

$$\nabla\psi.\nabla phi = \partial_x\psi\partial_x\phi + \partial_y\psi\partial_y\phi = -vu + uv = 0. \qquad (2.32)$$